

# Gravity and S-wave modelling across the Jan Mayen Ridge, North Atlantic; implications for crustal lithology

Rolf Mjelde · Inger Eckhoff · Ståle Solbakken · Shuichi Kodaira ·  
Hideki Shimamura · Karl Gunnarsson · Ayako Nakanishi · Hajime Shiobara

Received: 24 January 2005 / Accepted: 11 October 2006 / Published online: 26 January 2007  
© Springer Science+Business Media B.V. 2007

**Abstract** The horizontal components from fourteen Ocean Bottom Seismometers deployed along four profiles focused along the western margin of the Jan Mayen microcontinent, North Atlantic, have been modelled with regard to S-waves, based on P-wave models obtained earlier. The seismic models have furthermore been constrained by 2D gravity modelling. High  $V_p/V_s$ -ratios (2.3–7.9) within the Cenozoic sedimentary section are attributed to significant porosities, whereas  $V_p/V_s$ -ratios in the order of 1.9–2.2 for the Mesozoic and Paleozoic sedimentary rocks indicate shale-dominated lithology throughout the area. The eastern side of the Jan Mayen Ridge is interpreted as a passive, volcanic margin, based on relatively high crustal  $V_p/V_s$ -ratios (1.9), whereas lower  $V_p/V_s$ -ratios

(1.75–1.8) suggest the presence of intermediate composition crust and non-volcanic margin on the western side of the ridge. In the westernmost part of the Jan Mayen Basin, slightly increased upper mantle  $V_p/V_s$ -ratios may indicate some degree of serpentinization of upper mantle peridotites.

## Introduction

The Jan Mayen Ridge is a submarine structure extending southwards from the Jan Mayen Island in the North Atlantic (Fig. 1). The water depth at the crest of the ridge increases from north to south, with an average depth of c. 900 m. The c. 50 km wide Jan Mayen Basin, with water depths exceeding 2000 m, is located to the west of the ridge.

Earlier studies, involving gravity-, magnetic-, and seismic reflection measurements suggested continental origin of the ridge (Grønlie et al. 1979; Navrestad and Jørgensen 1979; Sundvor et al. 1979; Johansen et al. 1988). In this part of the Atlantic, seafloor spreading started at anomaly 24B (c. 55 Ma) along the Aegir Ridge, situated between the Jan Mayen Ridge and the Møre Margin, mid-Norway (e.g. Talwani and Eldholm 1977). Multichannel seismic data resolved an Early Tertiary basaltic sequence at the eastern flank of the ridge, and the eastern margin was subsequently interpreted as a passive volcanic margin by Myhre (1984) and Skogseid and Eldholm (1987).

The Aegir Ridge became extinct just prior to anomaly seven times (c. 25 Ma), when seafloor spreading commenced along the Kolbeinsey Ridge to

---

R. Mjelde (✉) · I. Eckhoff · S. Solbakken  
Department of Earth Science, University of Bergen, Allégt.  
41, 5007 Bergen, Norway  
e-mail: rolf.mjelde@geo.uib.no

S. Kodaira · H. Shimamura · A. Nakanishi ·  
H. Shiobara  
Institute of Seismology and Volcanology, Hokkaido  
University, Sapporo 060, Japan

*Present Address:*  
S. Kodaira *Present Address:*  
A. Nakanishi  
JAMSTEC, Natushima-cho 2-15, Yokosuka 237-0061, Japan

K. Gunnarsson  
National Energy Authority, Grensasvegi 9, 108, Reykjavik,  
Iceland

*Present Address:*  
H. Shiobara  
OHRC, Earthquake Research Institute, University of  
Tokyo, Yayoi 1-1-1, Bunkyo-ku 113-0032, Japan

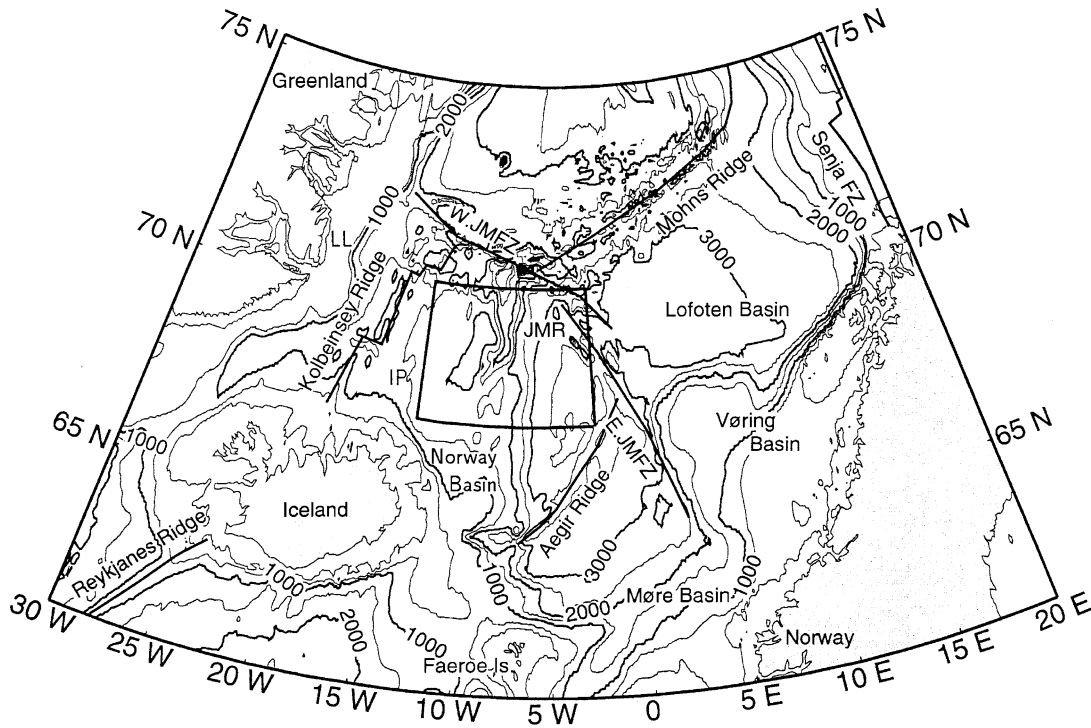
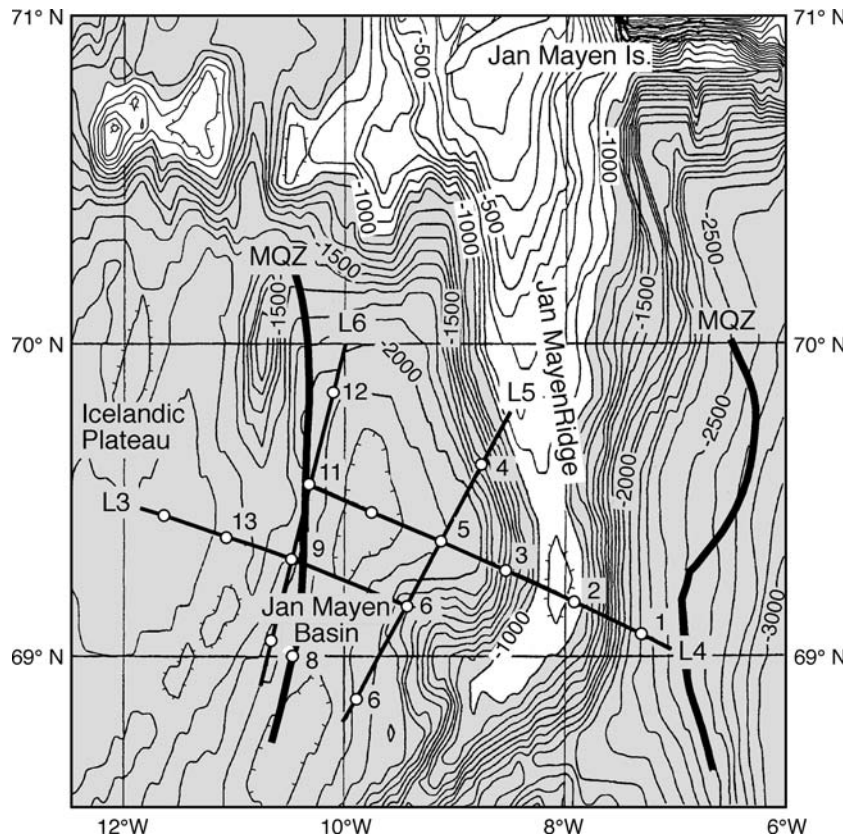


**Fig. 1** Regional physiography, simplified bathymetry and structural features of the Norwegian-Greenland Sea. LL = Liverpool Land, IP = Iceland Plateau, JMR = Jan Mayen Ridge,

JMFZ = Jan Mayen Fracture Zone. The study area is indicated by frame. Bathymetric contours in metres

**Fig. 2** Survey area with OBS profiles. L3, L4, L5 and L6 represent the acquired profiles, and numbers 1–14 indicate the OBS positions. MQZ: edges of magnetic quiet zone compiled by Olafsson (1983)



the west of the Jan Mayen Basin (Vogt et al. 1980). Kuvaas and Kodaira (1997) argued that continental stretching within East Greenland commenced at least 20 Myr before break-up occurred in the Jan Mayen Basin.

The P-wave modelling of a comprehensive Ocean Bottom Seismograph (OBS) dataset was presented by Kodaira et al. (1998; Fig. 2). Their modelling confirmed the continental origin of the Jan Mayen Ridge and Jan Mayen Basin, and strengthened the interpretation of the eastern margin as being volcanic. The modelling suggested, however, that the margin along the western flank of the ridge is non-volcanic. Furthermore, the modelling revealed that the oceanic crust formed shortly after break-up along the Kolbeinsey Ridge was 1.0–2.5 km thicker than normal due to influence from the Iceland Mantle Plume.

Elucidating the evolution of the Jan Mayen micro-continent is important for understanding the link between the early Tertiary North Atlantic Province and the Iceland Plume, and tectonomagmatic processes in general. The present paper discusses the modelling of gravity- and S-wave data, using the P-wave models presented by Kodaira et al. (1998) as basis. It is well established that gravity data can be used to support and refine P-wave velocity models, and that modelling of S-wave data, interpreted from OBS horizontal components, provides constraints on lithology and porosity (e.g. Mjelde et al. 2002a, b, 2003).

### Data acquisition and processing

In 1995, the universities of Bergen (Norway) and Hokkaido (Japan), in cooperation with the Icelandic National Energy Authority, performed an extensive geophysical survey in the Jan Mayen Ridge/Kolbeinsey Ridge area (Mjelde et al. 1995; Fig. 1). Locations of OBS profiles used in this study are shown in Fig. 2. Four profiles from the Iceland Plateau to the Jan Mayen Ridge were acquired mainly to determine the crustal structure beneath the ridge and the continent-ocean-transition along the western part of the ridge. The length of the two dip-profiles, L3 and L4, are about 100 and 140 km, respectively. In addition, two strike-profiles of 125 km length each (L5 and L6), were acquired along the eastern and western edge of the Jan Mayen Basin. Gravity data was acquired along all profiles using a LaCoste and Romberg sea gravity meter. The P-wave modelling of all profiles has been presented by Kodaira et al. (1998), and the S-wave modelling of L3 was discussed by Mjelde et al. (2002a). The present paper documents the S-wave and gravity

modelling of L4, L5 and L6, integrated with the results published earlier for the other profiles.

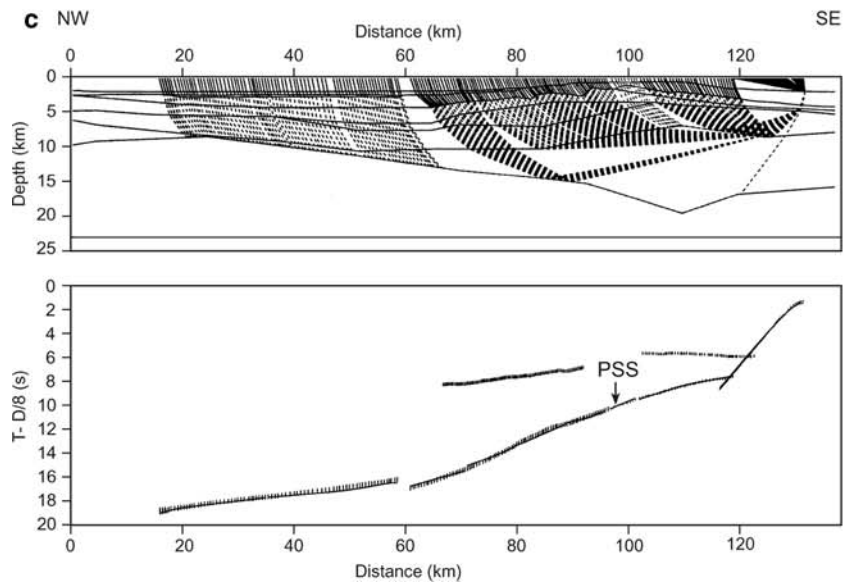
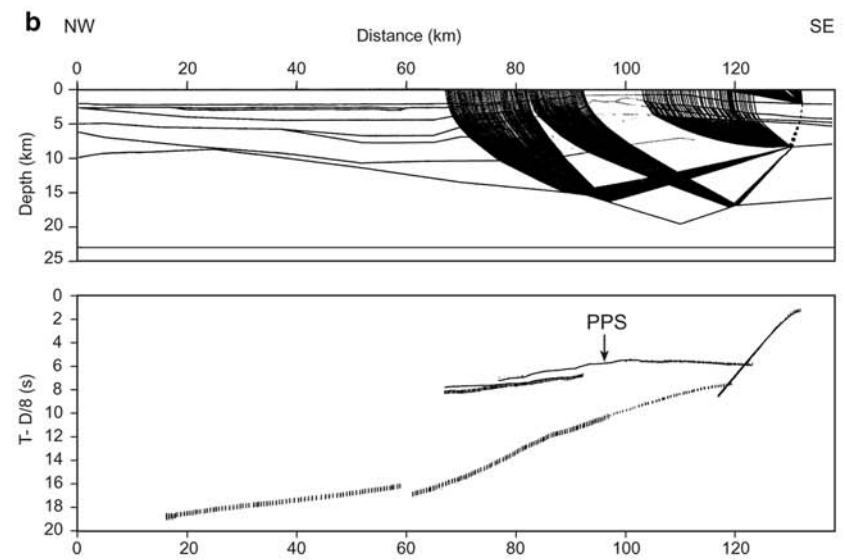
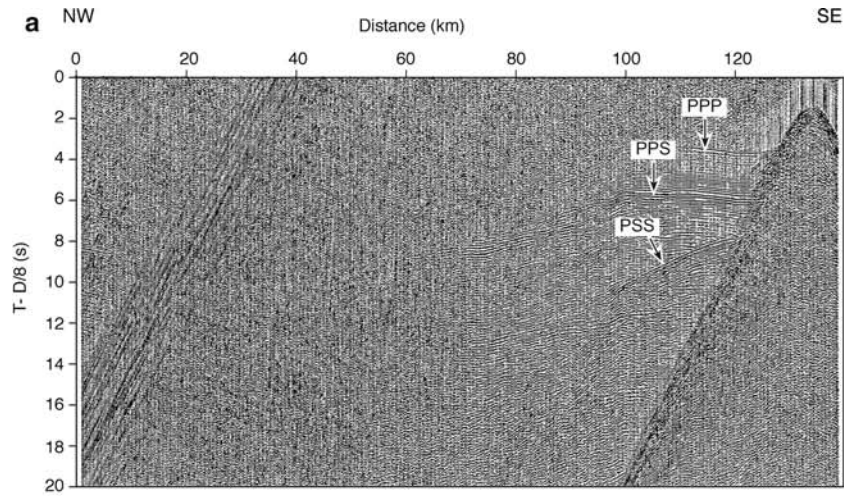
A total of 14 three-component OBSs were deployed along the four profiles, and single-channel reflection data were also acquired along all profiles. Parts of L4 and L5 were located on multichannel reflection profiles previously acquired by the Norwegian Petroleum Directorate. The OBSs used were equipped with three-component gimbal-mounted 4.5 Hz geophones. The instruments record continuously for 14 days within the 1–30 Hz frequency range (Kanazawa and Shiobara 1994). A tuned air-gun array consisting of six Bolt air-guns with a total volume of 2036  $\text{m}^3$  (33.4 l) were fired every minute at about 125 intervals along the profiles.

The analogue OBS data were digitized at Hokkaido University, and further processing was done at the University of Bergen. The 5–12 Hz bandpass-filtered data presented in this paper are scaled with an automatic gain control (AGC) window of 4.0 s and plotted with a reduction velocity of 8 km/s. The high reduction velocity is preferred since a significant portion of the S-wave arrivals are converted on the way up, and hence propagate with apparent P-wave velocity. Spiking deconvolution with 85 ms prediction distance and 2 s operator length was applied to the data, and FK filtering lead to clearer identification of some S-wave arrivals. The horizontal component data were rotated into in-line and cross-line components by use of the polarization of the direct water arrival. It is assumed that this can be done with an azimuthal uncertainty of  $\pm 5^\circ$  (Digranes et al. 1996). Only in-line component data are presented in this paper. Examples of such data are shown in Figs. 3–5.

### Modeling procedure

The starting model was derived by digitizing the most prominent reflections observed in the multichannel reflection (MCS) data available (Kodaira et al. 1998). The deepest reflection corresponds to Triassic strata on the Jan Mayen Ridge and the top of the magmatic crust westward of the Jan Mayen Basin. The model was subsequently depth converted using the P-wave velocity estimated from MCS interval velocities. The

**Fig. 3** (a) Horizontal component data from OBS 1, Line 4, plotted with 8 km/s reduction velocity, 5–12 Hz band-pass filtering and 4 s AGC window. PPP, PPS and PSS arrivals are indicated. (b) Ray-diagram, as well as interpreted (hatched) and calculated (solid) travel-time curves for the PPS arrivals. (c) Same as (b), for the PSS arrivals



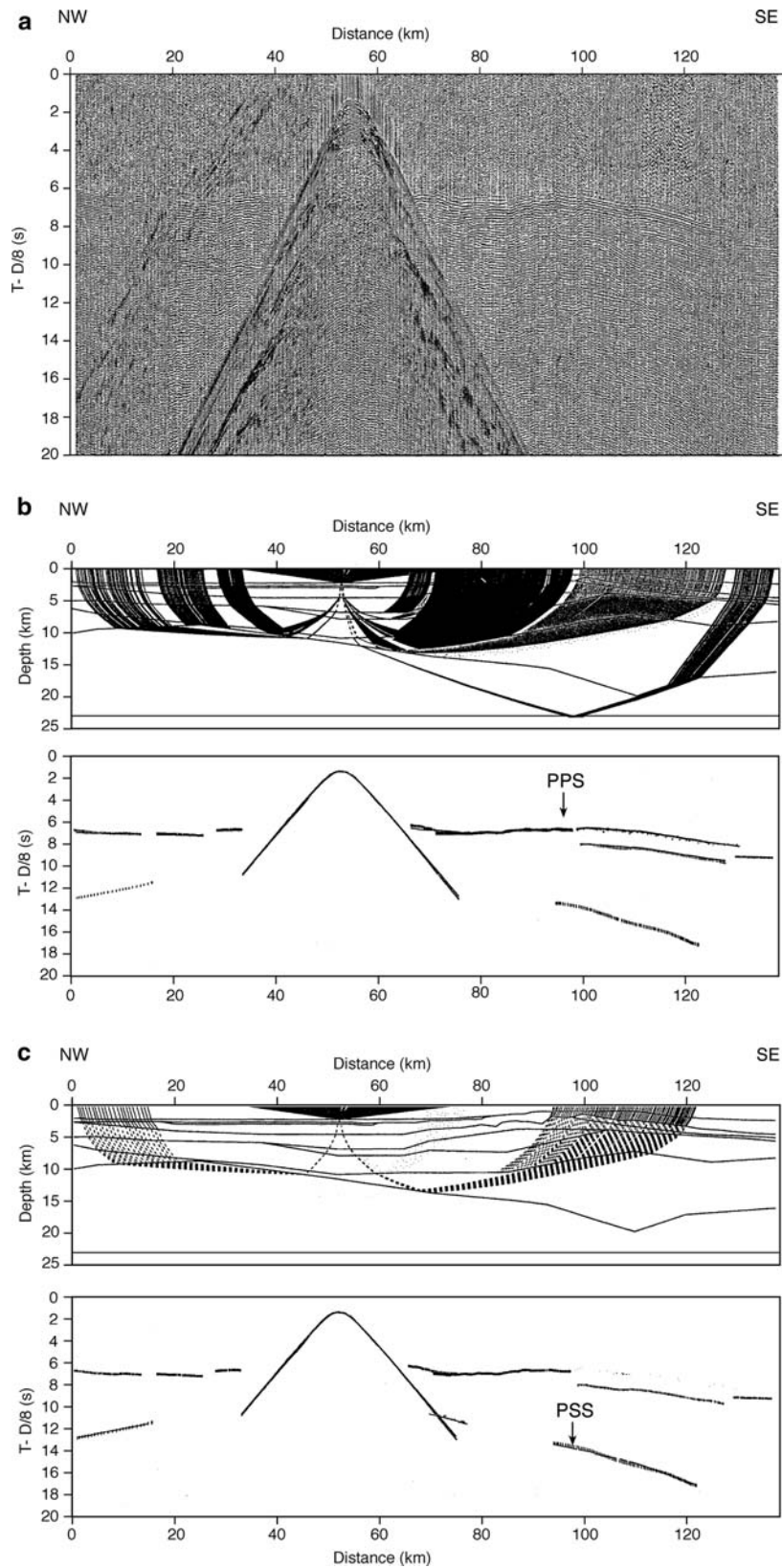


**Fig. 4** (a) Horizontal component data from OBS 5, Line 4, plotted with 8 km/s reduction velocity, 5–12 Hz band-pass filtering and 4 s AGC window. (b) Ray-diagram, as well as

interpreted (hatched) and calculated (solid) travel-time curves for the PPS arrivals. (c) Same as (b), for the PPS arrivals

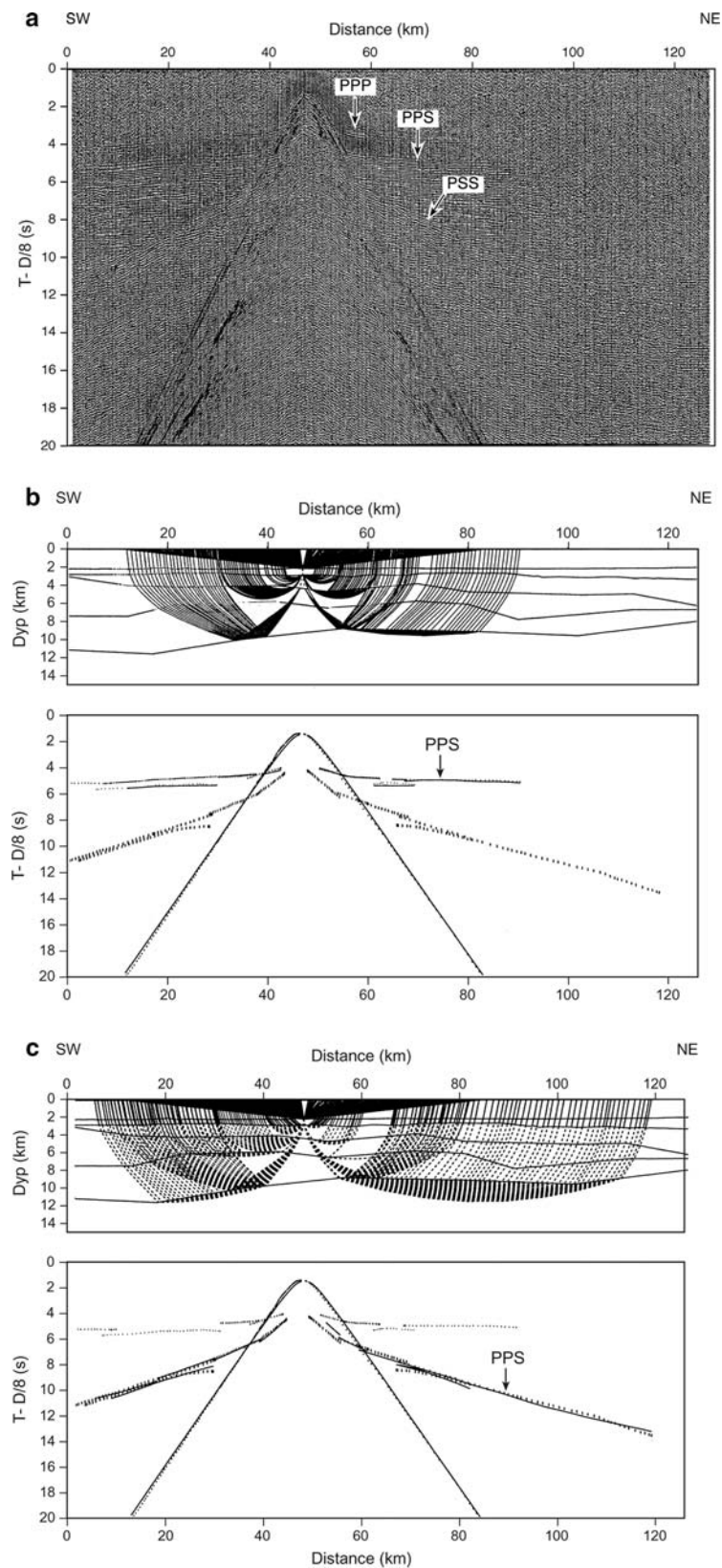


**Fig. 5** (a) Horizontal component data from OBS 9, Line 6, plotted with 8 km/s reduction velocity, 5–12 Hz band-pass filtering and 4 s AGC window. PPP, PPS and PSS arrivals are

indicated. (b) Ray-diagram, as well as interpreted (hatched) and calculated (solid) travel-time curves for the PPS arrivals. (c) Same as (b), for the PSS arrivals

modeling of the OBS-data was based on a combined inversion and forward modelling scheme (Zelt and Smith 1992). During the modelling, both velocities and interfaces were determined for successively deeper layers from the wide-angle reflections and refractions observed in the OBS-data. All layers have been modelled with both vertical and horizontal velocity gradients. The modeling of the P-wave data has been presented by Kodaira et al. (1998).

The seismic P-wave model was then tested by gravity modelling, which is presented here. For this purpose, the British Geological Survey Interactive 2.5D modelling program, GRAVMAG, was used. Average velocities within each layer provided initial density estimates by using the velocity-density relationship of Ludwig et al. (1970). The density was differentiated along each layer according to the velocity variations along the same layers.

The S-wave modelling, as discussed in the present paper, consisted of measuring the S-wave velocity (expressed as the  $V_p/V_s$ -ratio) for the different layers, using the same modelling software as for the P-waves, as well as determining the location of P-to-S conversion for each arrival. The observed arrivals can generally be classified in three groups depending on the depth of the conversion; PPS arrivals are converted on the way up, PSS are converted on the way down, and target converted waves are converted upon reflection, or at the top of the critical refractive interface. This modelling procedure is based on the assumption that an interface for P-waves corresponds to an interface for S-waves (Mjelde et al. 2002b). The PSS arrivals are most useful in the modeling, as they provide direct S-wave velocity estimates from the layer within which they refract critically. The PPS arrivals are useful in the sense that they provide independent estimates of the S-wave velocities above the interface of conversion.

### Basis for interpretation

In this section we describe the first-order geological interpretations that generally can be drawn from the type of models we derive. By first-order we mean “state-of-the-art” interpretations resulting from statistical averaging of well-studied field examples, related to borehole measurements of P-, and S-wave velocities and densities (e.g. Holbrook et al. 1992).

The P-wave velocity in sedimentary rocks primarily reflect their burial depth and history. The P-wave velocity in marine environments typically increases from 1.6–1.9 km/s near the sea-floor to 5.5–5.8 km/s at 10–15 km depth (e.g. Neidell 1985). A buried wedge of

volcanic extrusives commonly shows up as higher P-wave velocities than the surrounding sedimentary rock units; typically  $\approx 4.0$  km/s are observed near the top of the wedge, increasing to  $\approx 5.5$  near its base (e.g. White et al. 1992). The P-wave velocity in typical granitic/granodioritic crystalline crust increases from  $\approx 6.0$  km/s at the top to 6.6–6.9 km/s near the base of the crust (e.g. Holbrook et al. 1992). Lower crustal 7.2–7.6 km/s layers are generally interpreted as mafic intrusions/underplating (e.g. White and McKenzie 1989). Typical oceanic crustal layering corresponds to a sedimentary unit (1.6–3.0 km/s), layer 2A (pillow lavas; 4.0–4.5 km/s), layer 2B (sheeted dykes; 5.5–6.0 km/s), layer 3A (upper part of magma chamber; 6.5–6.9 km/s) and layer 3B (lower part of magma chamber; 7.1–7.5 km/s) (e.g. White et al. 1992). The Moho, generally interpreted as the crust-mantle boundary, represents a velocity jump to above  $\approx 7.7$  km/s (Holbrook et al. 1992). Unless otherwise stated, interfaces are observed both by refractive and reflective events, i.e. they represent first-order discontinuities in OBS-models.

The modeled densities are generally found to follow the velocity–depth relationships developed by Ludwig et al. (1970). Sedimentary densities are estimated to c.  $2.0 \text{ g/cm}^3$  near the sea-floor to c.  $2.75 \text{ g/cm}^3$  at 10–15 km depth. Typical crystalline, continental densities are in the order of  $2.85 \text{ g/cm}^3$ , increasing to  $3.0\text{--}3.2 \text{ g/cm}^3$  in mafic, lower crustal intrusive bodies. The upper mantle density is generally set to  $3.33 \text{ g/cm}^3$ .

$V_p/V_s$ -ratios above three are commonly observed in shallow marine sediments, and is generally attributed to low degree of compaction (Chung et al. 1990; Bromirski et al. 1992). It is well known that the increased confining pressure with depth leading to reduced porosity and closing of cracks, corresponds to decreasing  $V_p/V_s$ -ratios (Christensen and Mooney 1995; Sato and Ito 2001). The relationship between the  $V_p/V_s$ -ratio and lithology for well consolidated rocks, is established both from laboratory experiments and case studies (e.g. Neidell 1985; Tatham 1985; Tatham and McCormac 1991; Christensen 1996). Domenico (1984) used laboratory measurements to compute  $V_p/V_s$  ranges for common sedimentary lithologies and reported the following (pressure corrected) values; sandstones: 1.59–1.76, dolomite: 1.78–1.84, limestone: 1.84–1.99, shales: 1.70–3.00. The results indicate that sandstone represents the lower end-member, whereas shale generally corresponds to the higher values. The  $V_p/V_s$ -ratio is particularly sensitive to the content of quartz; while most rock forming minerals have  $V_p/V_s$ -ratios from 1.7 to 1.9, quartz has a value as low as 1.48 (Birch 1961). Hence, the  $V_p/V_s$ -ratio offers a means to distinguish between felsic (quartz rich) and mafic (quartz

poor) crystalline rocks. Holbrook et al. (1992) estimated  $V_p/V_s$ -ratios for different crystalline basement compositions, and found values that varied from 1.71 in granite (felsic) and 1.78 in granodiorite, to 1.84 in gabbro (mafic).

### The P-wave models

Since the S-wave and gravity modelling is based on the P-wave models discussed by Kodaira et al. (1998), we will briefly summarize their results, exemplified by the models of L3 and L4 (Fig. 6). The Cenozoic sedimentary rocks in the models are represented by the two uppermost layers, with maximum total thickness of c. 2 km in the Jan Mayen Basin (Fig. 6a). A thin high-velocity (4.6–5.0 km/s) basaltic intrusion is mapped in this basin. Based on interpretation of multichannel reflection data, Myhre et al. (1984) dated the intrusion to c. 30 Ma. On the Jan Mayen Ridge and eastwards, the modelling indicates a c. 1 km thick basaltic wedge,

inferred to be related to the Early Eocene continental break-up (Skogseid and Eldholm 1987).

The layer with Mesozoic sedimentary rocks is also thickest in the Jan Mayen Basin (max. 3 km), whereas the up to 3 km thick Paleozoic layer is restricted to a wedge beneath the western flank of the Jan Mayen Ridge. The succession of pre-Cenozoic rocks is very thin along the eastern flank of the ridge. The continental crystalline basement is divided in an upper layer with relatively uniform thickness of c. 4 km, and a lower layer which varies strongly in thickness, from absence in parts of the Jan Mayen Basin, to a maximum of 12 km beneath the Jan Mayen Ridge. No indications of lower crustal high-velocity layers (7 km/s), indicative of mafic underplating, were observed in the data. The depth to the Moho (top of the mantle) decreases from 20 km beneath the ridge to a minimum of c. 8 km in the Jan Mayen Basin. The modelling reveals a narrow continent-ocean-transition (c. 10 km), where velocities increases significantly westwards (Fig. 3b). The oceanic crust on the Icelandic Plateau is 1–2.5 km thicker than normal due to the elevated

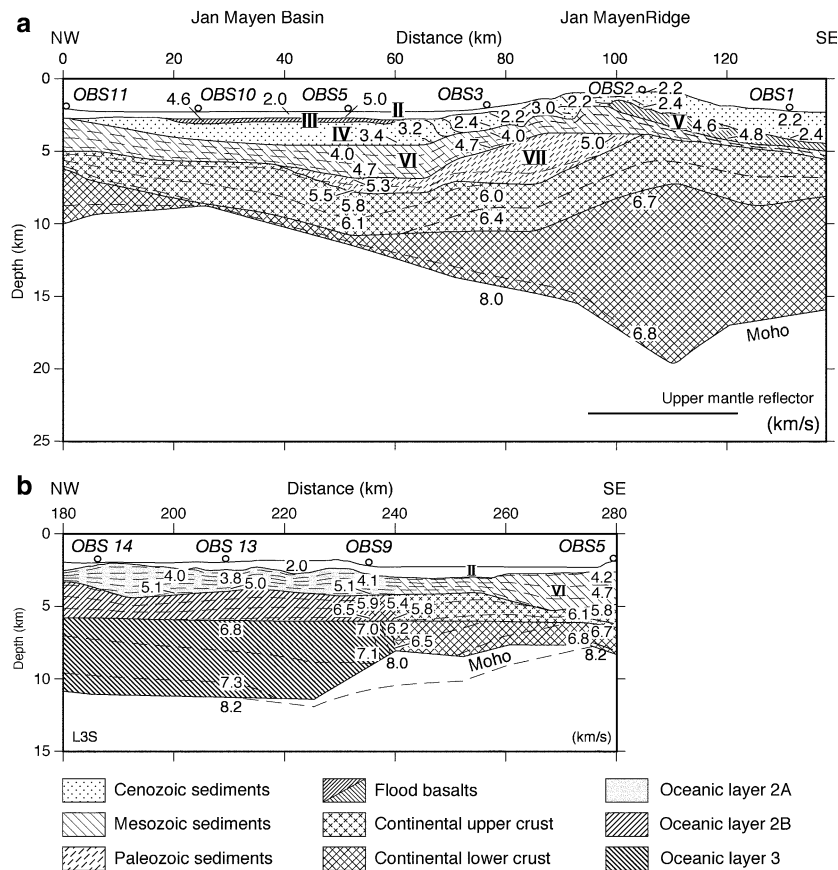


**Fig. 6 (a)** The P-wave velocity model for L4 across the Jan Mayen Ridge and Jan Mayen Basin with geological interpretation (from Kodaira et al. 1998). The numbers represent P-wave velocities (km/s) at the top and

bottom of the layers. The isovelocity contour interval is 0.2 km/s. **(b)** Same as **(a)** for L3, from the Jan Mayen Basin to the Iceland Plateau. See Fig. 2 for profile locations



mantle temperatures in the area (e.g. White and McKenzie 1989).

### Gravity modelling

Translating the P-wave velocity model into a density model faithful to the velocity–density relationship (Ludwig et al. 1970) results in a good fit for all parts of the model (Fig. 7), with exception of the upper mantle and the continental crust east of the Jan Mayen Ridge. The resolution for P-waves is not high enough to reveal lateral variations within the upper mantle, whereas the gravity modelling suggests significantly higher upper mantle densities in the southeastern part of the model (Fig. 7a). This may be interpreted as a thermal effect related to the progressively younger lithosphere northwestwards (Breivik et al. 1999). This effect is observed for several similar profiles across the conjugate mid-Norwegian margin (Mjelde et al. 2005; Breivik et al. 2006). The significant increase in crustal density on the eastern side of the Jan Mayen Ridge, from 2.82–2.91  $g/cm^3$  to 2.88–2.96  $g/cm^3$ , may suggest the presence of mafic intrusions in this part of the area, which was poorly imaged by the P-wave data. It must be underlined, however, that this anomaly close to the end of the profile possibly also may be explained by (unconstrained) structural variations further to the southeast. The misfit in modelled densities at line intersections can be attributed to offline effects. Note that the sharp (P-wave) continent-ocean-transition westwards is confirmed by lateral variations in modelled densities (Fig. 7c).

### S-wave modelling

The P-to-S conversions are generally found to occur at the interfaces with strongest impedance contrasts; e.g. for OBS 1, L4 (Fig. 3) the waves are converted at the top of the sedimentary intrusion in the Jan Mayen Basin, at the base Tertiary on the western side of the Jan Mayen Ridge and at the top of the Eocene basalt on the eastern side of the ridge. This pattern of conversions is consistent with observations from a comprehensive methodological survey presented by Mjelde et al. (2002b).

The  $V_p/V_s$ -ratios for the modelled profiles are presented in Fig. 8, and the average  $V_p/V_s$ -ratios for the different layers along each profile is shown in Table 1. The  $V_p/V_s$ -ratio is found to decrease with depth in the Cenozoic sedimentary section, where ratios within the range 2.3–7.9 are measured. The  $V_p/V_s$ -ratio cannot be

resolved for the thin intrusion in the Jan Mayen Basin, but the ratio is estimated to 1.85 for the Eocene basaltic sequence on the eastern side of the Jan Mayen Ridge. The  $V_p/V_s$ -ratio is measured to 1.9–2.2 in the Mesozoic layer and 1.9 in the Paleozoic sequence. Within the crystalline basement, the ratio is inferred to decrease from 1.8–1.9 in the upper layer to 1.7–1.8 in the lower crust. The same values are estimated for the upper mantle. The modelled  $V_p/V_s$ -ratios for the oceanic crust varies from a constant value of 1.75 for all layers along L3, to values decreasing with depth from 2.0 to 1.8 for L6.

### Modelling uncertainties and resolution

One advantage of the applied inversion scheme is that it has the potential of resolving the velocities and interface nodes used to construct the models, so that quantitative comparisons between the observed and calculated travel-times can be performed (e.g. Kodaira et al. 1997). The chi-squared value is weighing the mismatch between observed and calculated arrival times to the estimated uncertainty of the interpretation in such a way that a value of 1 or lower per phase signifies a reasonable fit (Zelt et al. 1992). This facilitates judging the quality of the interpretation, and it ought to ensure that the data is neither under- nor over-interpreted during the modelling. An example of  $\chi^2$  values for the different layers for an OBS is shown in Table 2. Such estimates should be used with care, since the uncertainties in the data picking (interpretation) remains unquantified during such comparisons. During the modelling of the profiles presented in this paper, the uncertainty of each interpreted branch of the travel-time curves has usually been kept at 50 ms, but the uncertainty of some of the crustal arrivals is higher; up to 200 ms. Note that several of the chi-squared values presented in Table 2 deviate significantly from 1. Such apparent misfits may be removed by carefully tuning the estimated uncertainty for each arrival to the calculated chi-squared value. We refrain from doing this in order to underline that the uncertainty in the interpretation remain unquantified. The resolution along the profiles is mainly a function of the distance between the OBSs (ray-coverage) and the data quality. The ray-coverage for L4 is shown in Fig. 9.

The gravity modelling is important in constraining the velocity models since it represents an independent, although non-unique, method. The gravity modelling is particularly important towards the ends of the profiles where the seismic resolution is zero.

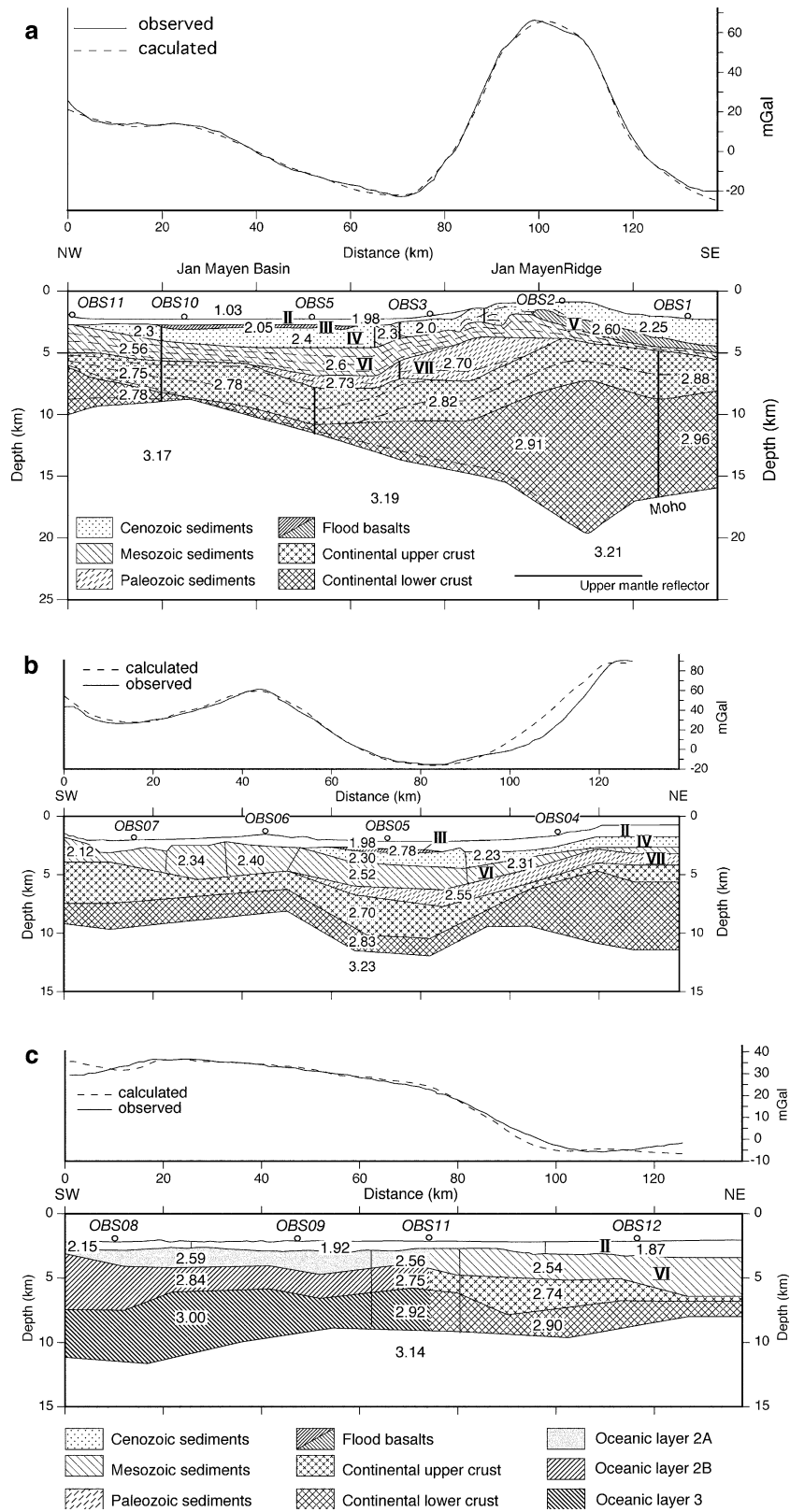


**Fig. 7** Gravity free-air observed and calculated anomalies, and the gravity model for Lines 4, 5 and 6 (shown in (a), (b) and (c), respectively). Densities in  $\text{g/m}^3$

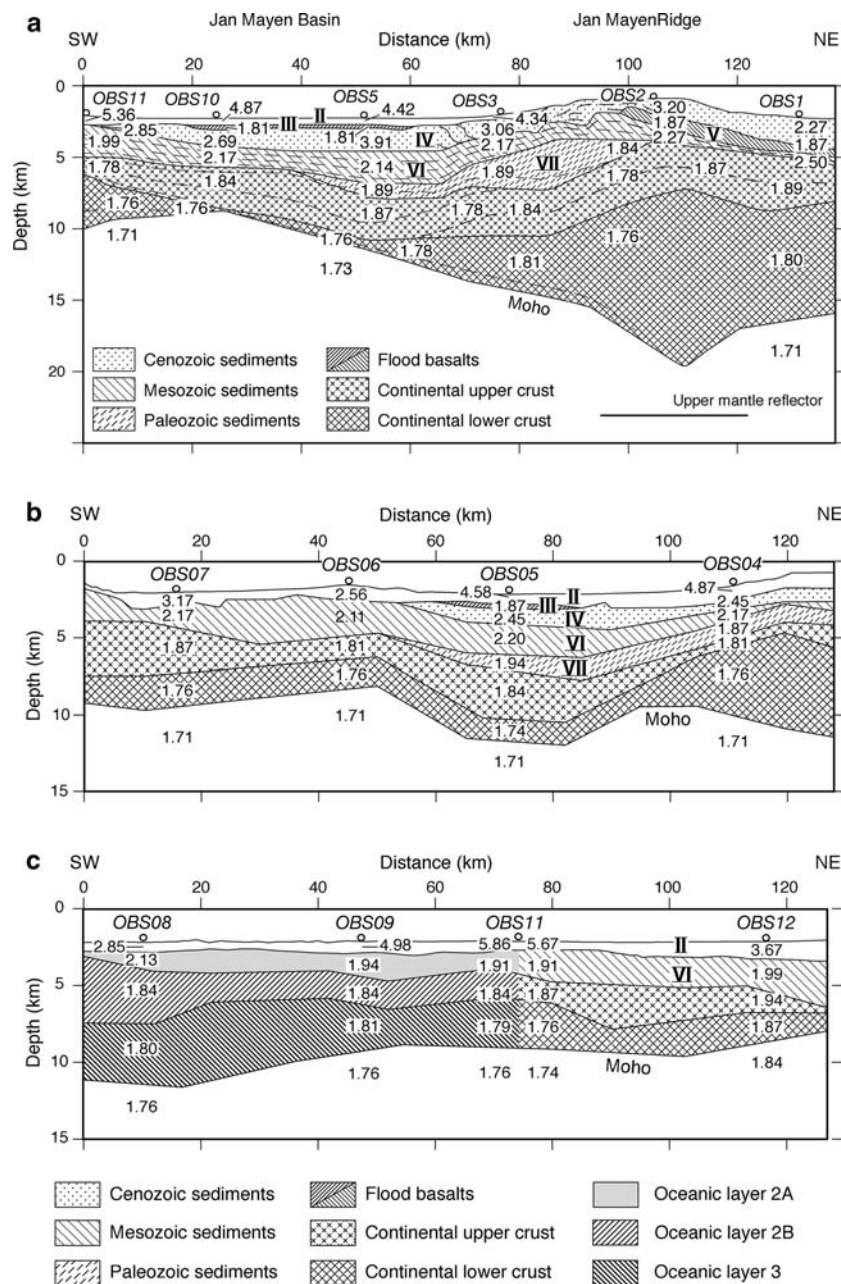


**Fig. 8** Final  $V_p/V_s$ -ratio models for Lines 4, 5 and 6 (shown in (a), (b) and (c), respectively)

The uncertainty in the S-wave modelling clearly depends on the uncertainty in the P-wave model (Kodaira et al. 1998). Based on their results and our observations we estimate the uncertainty in the  $V_p/V_s$ -ratio to be  $\pm 0.03$  in areas with high data quality (L6 and L4 at the Jan Mayen Ridge) and  $\pm 0.05$  in areas with moderate data quality (L5, and L4 off the Jan Mayen Ridge). These estimates are in agreement with more comprehensive, similar studies performed on the mid-Norwegian margin (e.g. Mjelde et al. 2003, 2005; Breivik et al. 2006).

The uncertainty described above can be referred to as the geophysical uncertainty. The geological uncertainty, related to how  $V_p/V_s$ -ratios are linked to some geologic parameter, is more difficult to quantify. It should be clear from the wide range of  $V_p/V_s$ -ratios vs lithology found in laboratory studies (e.g. Domenico 1984), that a certain picked  $V_p/V_s$ -ratio, as measured by our method, cannot be used directly to calculate, e.g. the sand/shale ratio at that location. The borehole confirmation of lithologies predicted from OBS data (e.g. Digranes et al. 1996), suggests,

**Table 2** Example of uncertainty estimate (OBS 3, L4, shotpoints to the southeast of the OBS)

Arrival	Nu. picks	rms (s)	uncert. (ms)	$\chi^2$	Converted
PPS	71	0.046	100	0.213	VII/VIII
	5	0.088	100	0.978	V/VI
	45	0.086	100	0.765	VI/VII
	44	0.102	100	1.074	VIII/IX
	20	0.050	100	0.265	VII/VIII
PSS	10	0.085	100	0.807	VIII/IX
	71	0.073	100	0.538	IV/V
	16	0.059	100	0.366	IV/V
	16	0.024	100	0.059	VI/VIII

The table shows from left to right the number of picks for each interpreted arrival, calculated rms-deviation from the picked arrivals, user-defined uncertainty, calculated chi-squared value (see text) and P-S converting interface for each arrival

**Table 1** Average  $V_p/V_s$ -ratios for each layer along the three modelled profiles

Layer number	L4	L5	L6	L3
I–IV (Cenozoic)	2.3–5.4	2.5–4.9	2.9–5.9	5.2–7.9
V (Eocene basalt)	1.85			
VI (Mesozoic)	2.2	2.15	1.95	1.9
VII (Paleozoic)	1.9	1.9		
Upper crust. crust	1.85	1.85	1.9	1.8
Lower crust. crust	1.80	1.75	1.8	1.7
Oceanic 2A			2.0	1.75
Oceanic 2B			1.85	1.75
Oceanic 3			1.8	1.75
Upper mantle	1.7	1.7	1.8	1.7

The results for L3 (Mjelde et al. 2002) are also included

however, that OBS-data can be used to predict regional trends in lithology variations, both laterally and with depth.

Based on this discussion and the results presented, the uncertainty in the depth to the main crustal layers and Moho is estimated to be  $\pm 0.5$  km in the areas where the coverage of rays and data quality is very good (L6 and L4 at the Jan Mayen Ridge),  $\pm 1.0$  km where the ray-coverage is poorer (L5, and L4 off the Jan Mayen Ridge), and  $\pm 1.5$  km close to the ends of the profiles. These estimates are in accord with the results from similar surveys and geological settings, as described by Mjelde et al. (2002a, 2003, 2005) and Digranes et al. (1996).

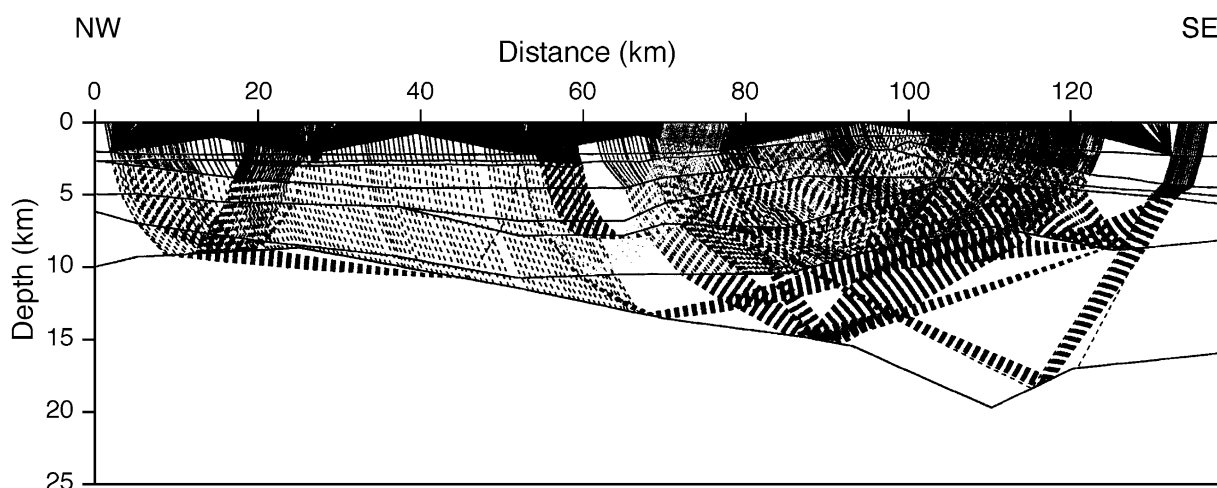
## Discussion

### Sedimentary layers

Based on the discussion above, we attribute the high  $V_p/V_s$ -ratios (2.3–7.9) observed in the Cenozoic sedimentary succession, to high porosity (Table 1). The relatively high  $V_p/V_s$ -ratios modelled for the Mesozoic and Paleozoic sedimentary rocks, 1.9–2.2 and 1.9, respectively, indicates shale-dominated lithology throughout the area. The  $V_p/V_s$ -ratio was estimated to 1.85 in the Eocene volcanic wedge, which is indicative of basaltic composition (e.g. Digranes et al. 1996).

### Continental crystalline crust

On the eastern side of the Jan Mayen Ridge the  $V_p/V_s$ -ratio is estimated to 1.9 in the upper crystalline crust, which indicates the presence of a significant portion of mafic intrusions (Fig. 8a). This is supported by increased modelled densities in the same area. Also note

**Fig. 9** Total ray-coverage for the PPS-arrivals along Line 4

that the PPS arrivals observed in OBS 1, L4 (Fig. 3) are dominantly converted on the top of the lower crust, which might be interpreted in terms of intrusions at these depths. The asymmetry of the Jan Mayen Ridge, with the largest crustal thickness on the eastern side of the ridge, may also be interpreted in terms of crustal growth due to mafic intrusions emplaced during the Eocene rifting and break-up (e.g. White and McKenzie 1989). The density and S-wave modelling thus support earlier studies that have referred to the eastern side of the Jan Mayen Ridge as a passive, volcanic margin.

Along the western side of the Jan Mayen Ridge and within the Jan Mayen Basin, the average  $V_p/V_s$ -ratio is estimated to 1.85 in the upper crystalline layer and 1.76 in the lower crust. Referring to the laboratory results described above, this could be interpreted as a dominantly mafic upper crystalline crust and a lower crust of intermediate composition. However, the crystalline P-wave velocities are significantly reduced in this part of the area; from above 6.0 km/s to 5.6–5.8 km/s in the upper crystalline crust (Fig. 6a). We agree with Kodaira et al. (1998), who interpreted this velocity decrease in terms of increased quantity of cracks. Crack porosity would increase the measured  $V_p/V_s$ -ratio, which should be corrected for this effect prior to lithology interpretations. The uncertainty of this correction is high, but based on the results discussed by Christensen and Mooney (1995), we estimate the effect on the  $V_p/V_s$ -ratio to be 0.05 for the upper crystalline crust. Applying this correction suggests intermediate composition throughout the crystalline crust. This interpretation is supported by observations from East Greenland, where uplifted and eroded crustal sections suggest dominantly felsic-intermediate composition (Henriksen et al. 2003). Our results thus support earlier studies that have indicated that the rifting between the Jan Mayen Ridge and East Greenland was non-volcanic (Weigel et al. 1995).

Kuvaas and Kodaira (1997) inferred that the rifting period west of the Jan Mayen Ridge was as long as 20–30 Myr. According to Bown and White (1995), such a long periode of rifting would imply conductive heat loss and insignificant generation of melts, even with asthenospheric temperatures risen at least 50° above normal.

#### Upper mantle

The  $V_p/V_s$ -ratio in the upper mantle is estimated to 1.7, which is consistent with peridotites (Holbrook et al. 1992). In the western part of the Jan Mayen Basin, close to the continent-ocean transition, the ratio is

modelled to be somewhat higher; 1.75–1.8. These higher values may indicate that the cracks inferred for the upper crystalline crust extend down to the upper mantle, and caused partially serpentization of the upper mantle peridotites. Such cracks were postulated by Kodaira et al. (1998), based on the slightly reduced upper mantle P-wave velocities modelled in this part of the area. This model implies penetration of seawater downwards through ca. 5 km of crust, which has been reported from oceanic crust elsewhere (Minshull et al. 1998). The observed decrease in P-wave velocities and increase in  $V_p/V_s$ -ratio implies c. 10% serpentization (Chian and Loudon 1994).

#### Oceanic crust

The S-wave modelling along the oceanic part of L3, performed by Mjelde et al. (2002a), indicated relatively low  $V_p/V_s$ -ratios for all crustal layers (1.75). These authors interpreted these results in terms of gabbroic composition, derived from a high-temperature melt with increased Mg content (White and McKenzie 1989). Christensen (1996) showed that increasing the Mg content at the expense of Fe will reduce the  $V_p/V_s$ -ratio.

The  $V_p/V_s$ -ratio modelled along the oceanic part of L6 indicates significantly higher values (1.8–2.0). These observations can be interpreted in terms of (normal temperature) gabbroic composition, with porosity increased  $V_p/V_s$ -ratio in oceanic layer 2A (2.0).

#### Summary and conclusions

Four OBS-profiles on the Jan Mayen Ridge, Jan Mayen Basin and across the continent-ocean-transition to the Icelandic Plateau have been modelled with regard to S-waves, supported by gravity modelling. The modelling was based on previous P-wave models along the same profiles, partly constrained by MCS-data.

The  $V_p/V_s$ -ratio is found to decrease with depth in the Cenozoic sedimentary section, where ratios within the range 2.3–7.9 are measured. These high values are attributed to significant porosities. The relatively high  $V_p/V_s$ -ratios modelled for the Mesozoic and Paleozoic sedimentary rocks, 1.9–2.2 and 1.9, respectively, indicates shale-dominated lithology throughout the area.

On the eastern side of the Jan Mayen Ridge the  $V_p/V_s$ -ratio is estimated to 1.9 in the upper crystalline crust, which indicates the presence of a significant portion of mafic intrusions. The eastern side of the Jan Mayen Ridge is hence interpreted as a passive, volcanic margin.

Along the western side of the Jan Mayen Ridge and within the Jan Mayen Basin, the average  $V_p/V_s$ -ratio is estimated to 1.85 in the upper crystalline layer and 1.76 in the lower crust. The crystalline P-wave velocities are significantly reduced by the presence of cracks in this part of the area; from above 6.0 km/s to 5.6–5.8 km/s in the upper crystalline crust. We estimate that adjusting for these cracks implies 0.05 reduction in the  $V_p/V_s$ -ratio before lithological interpretations can be made. Correcting for the cracks suggests intermediate composition throughout the crystalline crust. These results support earlier studies that have indicated that the rifting between the Jan Mayen Ridge and East Greenland was non-volcanic.

The  $V_p/V_s$ -ratio in the upper mantle is estimated to 1.7, which is consistent with peridotites. In the western part of the Jan Mayen Basin, close to the continent-ocean transition, the ratio is modelled to be somewhat higher; 1.75–1.8. These higher values may indicate that the cracks inferred for the upper crystalline crust extend down to the upper mantle, and caused partially serpentinization of the upper mantle peridotites. The gravity modelling suggests significant lateral decrease in upper mantle densities from southeast to northwest. This may be interpreted as a thermal effect related to the progressively younger lithosphere northwestwards.

**Acknowledgements** We thank the crew of R/V Håkon Mosby and the technical staff and students from the Department of Earth Science, University of Bergen, and the Laboratory for Ocean Bottom Seismology, Hokkaido University, for their support and skills during the acquisition of the data. We acknowledge Icelandic, Danish and Norwegian authorities for providing the necessary permits and information for the survey. A part of the survey was funded by the Ministry of Education, Science and Culture of Japan.

## References

- Birch F (1961) The velocity of compressional waves in rocks to 10 kilobars, Part 2. *J Geophys Res* 66:2199–2224
- Bown JW, White RS (1995) Effect of finite extension rate of melt generation at rifted continental margins. *J Geophys Res* 100:18011–18029
- Breivik AJ, Mjelde R, Faleide JJ, Murai Y (2006) Rates of continental breakup magmatism and seafloor spreading in the Norway Basin-Iceland Plume interaction. *J Geophys Res* 111(B07102):1–17
- Breivik AJ, Verhoef J, Faleide JJ (1999) Effect of thermal contrasts on gravity modelling at passive margins: results from the western Barents Sea. *J Geophys Res* 104:15293–15311
- Bromirski PD, Frazer LN, Dunnebie FK (1992) Sediment shear Q from airgun OBS data. *Geophys J Int* 110:465–485
- Chian D, Loudon KE (1994) The continent-ocean crustal transition across the southwest Greenland margin. *J Geophys Res* 99:9117–9135
- Christensen N (1996) Poissons's ratio and crustal seismology. *J Geophys Res* 101:3139–3156
- Christensen NI, Mooney WD (1995) Seismic velocity structure and composition of the continental crust: a global review. *J Geophys Res* 100:9761–9788
- Chung TW, Hirata N, Sato R (1990) Two-dimensional P- and S-wave velocity structure of the Yamato Basin, the southern Japan sea, from refraction data collected by an ocean bottom seismographic array. *J Phys Earth* 38:99–147
- Digranes P, Mjelde R, Kodaira S, Shimamura H, Kanazawa T, Shiobara H, Berg EW (1996) Modelling shear waves in OBS data from the Vøring Basin (Northern Norway) by 2-D ray-tracing. *Pure Appl Geophys* 4:611–629
- Domenico SN (1984) Rock lithology and porosity determination from shear and compressional wave velocity. *Geophysics* 49:1188–1195
- Grønlie G, Chapmann M, Talwani M (1979) Jan Mayen Ridge and Iceland Plateau: origin and evolution. *Norsk Polarinstittutt Skrift* 170:201–224
- Henriksen N, Higgins AK, Christoffersen M (2003) Caledonian Orogen East Greenland 70–82 N, a compilation of litho-structural data. The geological society of Denmark and Greenland, Copenhagen
- Holbrook WS, Mooney WD, Christensen NJ (1992) Seismic velocity structure of the deep continental crust. In: Fountain D, Arculus R, Kay RW (eds) *Continental lower crust*. Elsevier, Amsterdam, pp 451–464
- Johansen B, Eldholm O, Talwani M, Stoffa PL, Buhl P (1988) Expanding spread profile at the northern Jan Mayen Ridge. *Polar Res* 6:95–104
- Kanazawa T, Shiobara H (1994) Newly developed ocean bottom seismometer. Program Abstract, Japan Earth and Planetary Science Joint Meeting 341 (in Japanese)
- Kodaira S, Mjelde R, Gunnarsson K, Shiobara H, Shimamura H (1998) Structure of the Jan Mayen micro-continent and implications for its evolution. *Geophys J Int* 132:383–400
- Kodaira S, Mjelde R, Gunnarsson K, Shiobara H, Shimamura H (1997) Crustal structure of the Kolbeinsey Ridge, North Atlantic, obtained by use of ocean bottom seismographs. *J Geophys Res* 102:3131–3151
- Kuvaas B, Kodaira S (1997) The formation of the Jan Mayen microcontinent: the missing piece in the continental puzzle between the Møre-Vøring Basins and East Greenland. *First Break* 15(7):239–247
- Ludwig JW, Nafe JE, Drake CL (1970) Seismic refraction. In: Maxell AE (ed) *The Sea* 4. Wiley, New York, pp 53–84
- Minshull TA, Muller MR, Robinson CJ, White RS, Bickle MJ (1998) Is the oceanic Moho a serpentinization front? In: Mills RA, Harrison, K (eds) *Modern ocean floor processes and the geological record*. Geological Society, London, pp 71–80. Special Publication 148
- Mjelde R, Aurvåg R, Kodaira S, Shimamura H, Gunnarsson K, Nakanishi A, Shiobara H (2002a)  $V_p/V_s$ -ratios from the central Kolbeinsey Ridge to the Jan Mayen Basin, North Atlantic; implications on lithology, porosity and present-day stress field. *Marine Geophys Res* 23:125–145
- Mjelde R, Fjellanger JP, Raum T, Digranes P, Kodaira S, Breivik A, Shimamura H (2002b) Where do P-S conversions occur? Analysis of OBS-data from the NE Atlantic Margin. *First Break* 203:153–160
- Mjelde R, Kodaira S, Shimamura H (1995) OBS experiment Kolbeinsey Ridge - Jan Mayen Ridge, 2–21 May 1995, Cruise report, University of Bergen, 28 pp
- Mjelde R, Raum T, Digranes P, Shimamura H, Shiobara H, Kodaira S (2003)  $V_p/V_s$ -ratio along the Vøring Margin, NE

- Atlantic, derived from OBS-data: Implications on lithology and stress field. *Tectonophysics* 369:175–197
- Mjelde R, Raum T, Myhren B, Shimamura H, Murai Y, Takanami T, Karpuz R, Naess U (2005) Continent-ocean transition on the Vøring Plateau, NE Atlantic, derived from densely sampled ocean bottom seismometer data. *J Geophys Res* 110(B05101):1–19
- Myhre AM (1984) Compilation of seismic velocity measurements along the margins of the Norwegian-Greenland Sea. *Norsk Polarinstitutt Skrift* 180:46–67
- Myhre AM, Eldholm E, Sundvor E (1984) The Jan Mayen Ridge; present status. *Polar Res* 2:47–59
- Navrestad T, Jørgensen F (1979) Aeromagnetic investigations on the Jan Mayen Ridge. *Norwegian Petroleum Society NSS9*
- Neidell NS (1985) Land application of S waves. *Geophysics: The Leading Edge of Exploration* 11:32–44
- Sato H, Ito K (2001)  $H_2O$  fluid distribution in mantle rock at 1 GPa: constraints from  $V_s$ - $V_p/V_s$  diagram. *Bull Earthquake Res Inst Univ Tokyo* 76:305–310
- Skogseid J, Eldholm O (1987) Early Cenozoic crust at the Norwegian continental margin and the conjugate Jan Mayen Ridge. *J Geophys Res* 92:11471–11491
- Sundvor E, Gidskehaug A, Myhre AM, Eldholm O (1979) Marine geophysical survey on the northern Jan Mayen Ridge. Seismological observatory, University of Bergen, Scientific report 6
- Talwani M, Eldholm O (1977) Evolution of the Norwegian-Greenland Sea. *Geol Soc Am Bull* 88:969–999
- Tatham RH (1985) Shear waves and lithology. In: Dohr G (ed) *Seismic shear waves, part b: applications*. Geophysical Press, London-Amsterdam, pp 86–133
- Tatham RH, McCormac MD (1991) Rock physics measurements. In: Neitzel EB, Winterstein DF (eds) *Multicomponent seismology in petroleum exploration*. SEG investigation in geophysics series 6, pp 43–91
- Vogt PG, Johson GL, Kristjansson L (1980) Morphology and magnetic anomalies North of Iceland. *J Geophys* 47:67–80
- Weigel W, Flueh ER, Miller H, Butzke A, Deghani GA, Gebhardt V, Harder I, Hepper J, Jokat W, Klaschen D, Kreyman S, Schussler, S, Zhao Z (1995) Investigations of the East Greenland Continental Margin between 70 and 72 N by deep seismic sounding and gravity studies. *Marine Geophys Res* 17:167–199
- White RS, McKenzie D (1989) Magmatism at rift zones: The generation of volcanic continental margins and flood basalts. *J Geophys Res* 94:7685–7729
- White RS, McKenzie D, O' Nions RK (1992) Oceanic crustal thickness from seismic measurements and rare earth element inversions. *J Geophys Res* 97: 19683–19715
- Zelt CA, Smith RB (1992) Seismic traveltime inversions for 2-D crustal velocity structure. *Geophysical. J Int* 108:16–34